REAL vs. COMPLEX BPSK PRECODING FOR MIMO BROADCAST CHANNELS

Rodrigo de Miguel and Ralf. R. Müller
Department of Electronics and Telecommunications
Norwegian University of Science and Technology
7491 Trondheim, Norway
Email: {demiguel, ralf}@iet.ntnu.no

***Abstract*—Recently Müller *et al.* (*IEEE J. Select. Areas Commun.* 2008) used asymptotic methods from statistical physics to analyze non-linear vector precoding for MIMO broadcast channels. They proposed to extend BPSK input alphabets onto both real and complex supersets of the original constellation points. They showed that, as the optimization space is greater, lower energies are achieved when the extended alphabets are complex. In this work we use similar asymptotic methods and propose an alternative channel inversion technique which makes purely real alphabets perform as well as their complex extensions, which results in reduced complexity in the optimization process.**

I. Introduction

In multiple-input/multiple-output (MIMO) channels information is conveyed simultaneously from a group of transmitting antennas to a group of receiving antennas. As these transmissions are not orthogonal, yet they occur over the same physical medium and bandwidth, crosstalk becomes unavoidable. As a result signal processing needs to be done at the receiver and/or transmitter side of the channel if significant data rates are to be achieved. In the context of low cost receivers with limited processing power and battery life, it might be advantageous to shift most of the signal processing to the transmitter side.

In the case of a MIMO broadcast channel, the receiving antennas are at different locations, which means that they might not jointly process the data they independently receive. The transmitting antennas, however, are collocated and they jointly generate the data streams to be transmitted to each of the single receiving antennas, also known as users. One technique which might be employed by the transmitter in order keep the users from doing any signal processing is channel inversion before transmission (provided that the transmitter has complete channel state information). Unfortunately, plain channel inversion at the transmitter comes at an increased transmission energy cost. One technique which may be used to contain the transmit power while inverting the channel is non-linear vector precoding (henceforth vector precoding) [1], [2]. The vector precoding technique, outlined in Section II, consists of extending the input alphabets representing different information states; this permits the search for symbols which draw less energy when transmitted with channel inversion.

Müller et al. [3] used the replica method of statistical physics to analyze vector precoding in asymptotic MIMO channels. They proposed to extend binary phase-shift keying (BPSK) input alphabets onto both real and complex supersets of the original constellation points. They showed that, as the optimization space is greater, lower energies are achieved when the extended alphabets are complex.

Tulino and Verdu [4] and Lampe and Breiling [5] proposed linear receivers for BPSK direct-sequence code-division multiple access (DS-CDMA) which jointly process the received signal and its complex conjugate. In [6] Schober et al. showed that the real part of the matched filter output gives sufficient statistics for multiuser detection of DS-CDMA with real-valued modulation schemes.

In this work we propose an alternative channel inversion technique which might be used for purely real input alphabets. We use the replica method to show that this alternative channel inversion technique allows non-linear precoding with purely real alphabets to result in transmitted energies not greater than with complex alphabets. This occurs even when the real optimization space is a subset of the complex optimization space, leading to a reduction in complexity. Although the results presented here apply to any real-valued modulation scheme we concentrate on BPSK for simplicity.

II. Vector precoding

The MIMO broadcast channel may be represented by the following vector equality:

$$\mathbf{r} = \frac{1}{\sqrt{N}}\mathbf{H}\mathbf{t} + \mathbf{n}, \tag{1}$$

where $\mathbf{t}$ is the N-dimensional input to the channel, $\mathbf{r}$ is a vector containing the K received data streams, $\mathbf{n}$ is a random vector containing additive noise components, and the channel matrix $\mathbf{H}$ is a complex rectangular matrix which can be written as $\mathbf{H} = \mathbf{H}_r + \mathrm{j}\mathbf{H}_i$, where $\mathbf{H}_r$ and $\mathbf{H}_i$ are real random matrices containing independent and identically distributed entries with zero mean and variance $1/2$.

The transmitted vector $\mathbf{t}$ is a $N-$dimensional linear transformation of the K information symbols (contained in $\mathbf{x}$)

This work was supported by the Research Council of Norway (Grant 171133/V30).

978-1-4244-2644-7/08/$25.00 ©2008 IEEE

intended for the K users, thus we might write

$$\mathbf{t} \equiv \mathbf{T}\mathbf{x}. \tag{2}$$

In order to guarantee individual detection by the receivers, the transmitter, who has complete channel state information, might construct $\mathbf{T}$ such that, before modulo reduction, the information symbols in $\mathbf{x}$ can be received interference free (up to additive noise) by a simple diagonal (though not necessarily linear) operation $\hat{\Omega}$ on $\mathbf{r}$:

$$\hat{\Omega}\mathbf{r} = \mathbf{x} + \hat{\Omega}\mathbf{n}. \tag{3}$$

Using this transmission scheme, the transmitted energy per symbol is given by

$$K^{-1}\mathbf{t}^{\dagger}\mathbf{t} = K^{-1}\mathbf{x}^{\dagger}\mathbf{E}\mathbf{x}, \tag{4}$$

where the energy metric $\mathbf{E}$ is given by

$$\mathbf{E} = \mathbf{T}^{\dagger}\mathbf{T}. \tag{5}$$

A. Channel inversion

The $K \times K$ matrix $\mathbf{H}\mathbf{H}^{\dagger}$ has rank given by $\min\{N, K\}$. The inverse of $\mathbf{H}\mathbf{H}^{\dagger}$ only exists when $K < N$. A channel is said to be overloaded when there are more receiving users than there are antennas at the transmitter, *i.e.* $K > N$. In order to allow for the possibility of inverting overloaded channels, the transmitter might employ the generalized channel inversion technique outlined in the following.

When a matrix $\mathbf{M}$ is hermitian, as is $\mathbf{H}\mathbf{H}^{\dagger}$, we might write

$$\mathbf{M} = \mathbf{U}\mathbf{\Lambda}\mathbf{U}^{\dagger}, \tag{6}$$

where $\mathbf{U}$ is a unitary matrix and $\mathbf{\Lambda} \equiv \text{diag}\left(\lambda_{\mathbf{1}}, \lambda_{\mathbf{2}}, \cdots, \lambda_{\mathbf{K}}\right)$ is a diagonal matrix containing the K eigenvalues of $\mathbf{M}$. We might then define the pseudoinverse of $\mathbf{M}$ as

$$\mathbf{M}^{\widetilde{-1}} = \mathbf{U}\mathbf{\Lambda}^{\widetilde{-1}}\mathbf{U}^{\dagger}, \tag{7}$$

where

$$\mathbf{\Lambda}^{\widetilde{-1}} \equiv \lim_{\epsilon \to \mathbf{0}} \text{diag}\left(\frac{\mathbf{1} - \delta_{\lambda_{\mathbf{1}},\mathbf{0}}}{\lambda_{\mathbf{1}} + \epsilon}, \frac{\mathbf{1} - \delta_{\lambda_{\mathbf{2}},\mathbf{0}}}{\lambda_{\mathbf{2}} + \epsilon}, \cdots, \frac{\mathbf{1} - \delta_{\lambda_{\mathbf{K}},\mathbf{0}}}{\lambda_{\mathbf{K}} + \epsilon}\right) \tag{8}$$

and $\delta_{i,j}$ is the Kronecker delta. Note that $\mathbf{M}^{\widetilde{-1}}$ is nothing but the Moore-Penrose inverse of the square matrix $\mathbf{M}$.

1) Complex symbol mapping: If the symbols used to map the data are complex, *i.e.* $\mathbf{x} \in \mathbb{C}^K$, and the K-dimensional complex data vector $\mathbf{x}$ lies in the $\min\{N, K\}$-dimensional space spanned by $\mathbf{H}\mathbf{H}^{\dagger}$, denoted as $\mathcal{S}_{\mathbf{H}}$, then the matrix $\mathbf{T}$ and the diagonal operator $\hat{\Omega}$ can be constructed as follows:

$$\mathbf{T} \to \mathbf{T}_{\mathcal{C}} \equiv \frac{\mathbf{H}^{\dagger}}{\sqrt{N}}\left(\frac{\mathbf{H}\mathbf{H}^{\dagger}}{N}\right)^{\widetilde{-1}}, \tag{9}$$

$$\hat{\Omega} \to \hat{\Omega}_{\mathcal{C}} \equiv \mathbf{I}. \tag{10}$$

Then the transmitted energy per symbol is given by

$$K^{-1}\mathbf{t}^{\dagger}\mathbf{t} = K^{-1}\mathbf{x}^{\dagger}\mathbf{E}_{\mathcal{C}}\mathbf{x}, \tag{11}$$

where

$$\mathbf{E}_{\mathcal{C}} \equiv \mathbf{T}_{\mathcal{C}}^{\dagger}\mathbf{T}_{\mathcal{C}} = \left(\frac{\mathbf{H}\mathbf{H}^{\dagger}}{N}\right)^{\widetilde{-1}}. \tag{12}$$

Evidently, when the K-dimensional complex data vector $\mathbf{x}$ does not lie in $\mathcal{S}_{\mathbf{H}}$ no vector can be transmitted.

2) Real symbol mapping: If, on the other hand, only purely real symbols are used to map the data for the K users, *i.e.* $\mathbf{x} \in \mathbb{R}^K$, then the matrix $\mathbf{T} \to \mathbf{T}_{\mathcal{R}} = \mathbf{T}_r + \text{j}\mathbf{T}_i$ and the diagonal operator $\hat{\Omega}$ might be constructed in an alternative fashion:

$$\begin{bmatrix}\mathbf{T}_r \\ \mathbf{T}_i\end{bmatrix} \equiv \frac{1}{\sqrt{N}}\begin{bmatrix}\mathbf{H}_r^{\mathrm{T}} \\ -\mathbf{H}_i^{\mathrm{T}}\end{bmatrix}\left\{\Re\left(\frac{\mathbf{H}\mathbf{H}^{\dagger}}{N}\right)\right\}^{\widetilde{-1}}, \tag{13}$$

$$\hat{\Omega} \to \hat{\Omega}_{\mathcal{R}} \equiv \Re, \tag{14}$$

where $\Re$ is the *real-part* operator. Under this transmission scheme, the transmitted energy per symbol is given by

$$K^{-1}\mathbf{t}^{\dagger}\mathbf{t} = K^{-1}\mathbf{x}^{\dagger}\mathbf{E}_{\mathcal{R}}\mathbf{x}, \tag{15}$$

where

$$\mathbf{E}_{\mathcal{R}} \equiv \mathbf{T}_{\mathcal{R}}^{\dagger}\mathbf{T}_{\mathcal{R}} = \left\{\Re\left(\frac{\mathbf{H}\mathbf{H}^{\dagger}}{N}\right)\right\}^{\widetilde{-1}}. \tag{16}$$

The reason for introducing a separate channel inversion technique for the case of purely real information symbols will become apparent later. But it is important to note that, as opposed to Eq. (12), the matrix whose pseudoinverse is taken in Eq. (16) becomes rank deficient only when $K > 2N$.

B. Minimizing the transmitted energy

Although channel inversion by the transmitter keeps the users from having to process any interference, it might come at the cost of a high transmission energy. The goal of the vector precoding technique is minimizing the cost of the channel inversion process, *i.e.* minimizing Eq. (4). For this purpose, it is agreed between the transmitter and the users that, although there must be a minimum distance between any two symbols representing different information states, each state might be represented by more than one symbol. This gives the transmitter greater freedom to construct the information vector $\mathbf{x}$ with symbols which faithfully represent the intended information, yet they are chosen so as to minimize Eq. (4).

The information which the transmitter intends for user k is the state s_k. The symbols which might represent the state s_k are those contained in the set $\mathcal{A}_{s_k}$. Then the K-dimensional vector $\mathbf{x}$ can be constructed with components $\{x_1 \in \mathcal{A}_{s_1}, \cdots, x_K \in \mathcal{A}_{s_K}\}$, or, in short $\mathbf{x} \in \mathcal{A}$, where $\mathcal{A} = \mathcal{A}_{s_1} \times \mathcal{A}_{s_2} \times \cdots \times \mathcal{A}_{s_K}$. The transmitter chooses the symbol representation in $\mathcal{A} \cap \mathcal{S}_{\mathbf{H}}$ which minimizes the transmitted energy:

$$\mathbf{x} \equiv \underset{\tilde{\mathbf{x}} \in \mathcal{A} \cap \mathcal{S}_{\mathbf{H}}}{\arg\min} K^{-1}\tilde{\mathbf{x}}^{\dagger}\mathbf{E}\tilde{\mathbf{x}}. \tag{17}$$

In Sections IV and V we introduce different alphabet relaxation schemes for transmitting 1 or 2 uncoded bits to each user. When the alphabets representing the different information states are convex, then efficient algorithms might be used to find the optimal $\mathbf{x}$. However, if the symbol alphabets are discrete, then $\mathbf{x}$ can only be found performing an exhaustive search, which becomes prohibitively expensive when the number of users is large or the alphabet contains many symbols.

III. The transmitted energy

The technique outlined in Section II describes how to minimize the transmitted energy while achieving interference-free and individual reception by the users. In this section the expression for the transmitted energy per symbol using this transmission technique is presented. First, one might note that the transmitted energy per symbol E might be written as

$$E \equiv \min_{\mathbf{x}\in\mathcal{A}\cap\mathcal{S}_{\mathbf{H}}} K^{-1}\mathbf{x}^\dagger\mathbf{E}\mathbf{x} = = -\beta^{-1}K^{-1}\lim_{\beta\to\infty}\ln\sum_{\mathbf{x}\in\mathcal{A}\cap\mathcal{S}_{\mathbf{H}}} \mathrm{e}^{-\beta\mathbf{x}^\dagger\mathbf{E}\mathbf{x}}. \quad (18)$$

The right hand side of (18) has the same form as the expression for the Helmholtz free energy of a thermodynamic system with temperature $1/\beta$ [7]. In the following we take advantage of this fact by taking a thermodynamic approximation, *i.e.* we always assume that K and N are infinitely large[1], yet they have a finite ratio $\alpha = K/N$. This approximation will allow us to make use of mathematical tools imported from the statistical physics literature.

Using the replica method of spin glass theory [8] and assuming replica symmetry, we shown (in a later contribution due to space limitations) that, in the thermodynamic limit, the energy (18) is fully determined by the eigendistribution of $\mathbf{E}$, and the information symbol alphabets. The resulting expression for the energy per transmitted symbol is the following self-consistent equation:

$$E = \frac{\sum_i P_i\int_{\mathbb{C}}\left|\underset{\xi\in\mathcal{A}_i}{\arg\min}\left|z-\frac{\xi}{\sqrt{\alpha E}}\right|\right|^2 \mathrm{D}z}{1-\frac{\alpha\tau}{2}+2\sqrt{\frac{\alpha}{E}}\sum_i P_i\Re\int_{\mathbb{C}}\underset{\xi\in\mathcal{A}_i}{\arg\min}\left|z-\frac{\xi}{\sqrt{\alpha E}}\right| z^*\mathrm{D}z}, \quad (19)$$

where $\mathrm{D}z \equiv \frac{\mathrm{e}^{-|z|^2}}{\pi}\mathrm{d}z$. The index i denotes the different information states, each of which can be represented by elements in the set $\mathcal{A}_i$ and occurs in the components of $\mathbf{x}$ with probability P_i. The parameter τ equals 1 when $\mathbf{E} = \mathbf{E}_{\mathcal{R}}$ and it equals 2 when $\mathbf{E} = \mathbf{E}_{\mathcal{C}}$. [2]

An important assumption which was made in the derivation of Eq. (19) was that of replica symmetry. Although this approximation generally yields only a lower bound to the energy, it is commonly used in the analysis of magnetic and neural systems exhibiting quenched interactions often yielding excellent agreement with exact and numerical results (see *e.g.* [9]). Indeed replica symmetry has been successfully applied to problems in wireless communications (see *e.g.* [10]–[13]) and coding theory (see *e.g.* [14], [15]). In Section VI we show that, here too, the replica symmetric assumption mimics finite size results if the alphabets representing the different information states are convex.

[1]As we shall see in Section VI, this asymptotic channel limit can, in some cases, be a fair approximation for systems as small as $N = 10$.

[2]The derivation for the special case of $\tau = 2$ may already be found in [3].

IV. Alphabet relaxation for binary phase shift keying (BPSK)

We consider a source of information consisting of two equiprobable states: $\uparrow$ and $\downarrow$. When no vector precoding is employed the entries in $\mathbf{x}$ are usually selected from the unit BPSK alphabets $\mathcal{A}_\uparrow = \{+1\}$ and $\mathcal{A}_\downarrow = \{-1\}$. So long as the minimum distance between two points representing different information states is preserved, points might be added to these sets with the aim of reducing the transmitted energy.

In this section we propose different continuous and discrete alphabet extension schemes. While some of these alphabets are purely real, others allow for complex symbols to map the information states. As outlined in Section II, when the symbols used to map the information states are purely real then we might use any of the two different vector precoding schemes, whose resulting energy metrics are either $\mathbf{E}_{\mathcal{C}}$ or $\mathbf{E}_{\mathcal{R}}$. However, when the symbols used to map the information are complex, only the technique resulting in $\mathbf{E}_{\mathcal{C}}$ might be used. The parameter τ, remember from Section III, equals 1 when the energy metric is $\mathbf{E}_{\mathcal{R}}$, or 2 when it is $\mathbf{E}_{\mathcal{C}}$. Therefore, when the alphabet under consideration contains complex entries we will automatically set $\tau = 2$, whereas for purely real alphabets τ can take any of both values, depending on the channel inversion technique to be employed. The difference between both choices is further explored in Section VI.

A. Binary real convex relaxation

A trivial way to relax BPSK onto the real line is as follows:

$$\mathcal{A}_\uparrow = -\mathcal{A}_\downarrow = \{\xi : \xi \geq 1\}. \quad (20)$$

This relaxed alphabet, shown in Fig. 1.*a*, yields, after (19), the following expression for the energy per transmitted symbol:

$$E = \frac{2+\sqrt{\frac{\alpha E}{\pi}}\mathrm{e}^{-\frac{1}{\alpha E}}+\{\alpha E-2\}\,Q\left(\sqrt{2/\alpha E}\right)}{2-\tau\alpha+2\alpha Q\left(\sqrt{2/\alpha E}\right)}, \quad (21)$$

where the function $Q(\cdot)$ is defined as

$$Q(\sigma) \equiv \frac{1}{\sqrt{2\pi}}\int_\sigma^\infty \mathrm{e}^{-\frac{t^2}{2}}\mathrm{d}t. \quad (22)$$

B. Binary complex convex relaxation

The real relaxation space introduced in Section IV-A might be further extended onto the complex plane as follows:

$$\mathcal{A}_\uparrow = -\mathcal{A}_\downarrow = \{\xi \in \mathbb{C} : \Re\xi \geq 1\}. \quad (23)$$

As the information states are now mapped onto complex symbols, we might only use the channel inversion scheme resulting in the energy metric (12), which has complex entries. Therefore the parameter τ will now be equal to 2. Under this precoding scheme, shown in Fig. 1.*c*, Eq. (19) becomes

$$E = \frac{2+\sqrt{\frac{\alpha E}{\pi}}\mathrm{e}^{-\frac{1}{\alpha E}}+\{\alpha E-2\}\,Q\left(\sqrt{2/\alpha E}\right)+\alpha E}{2+2\alpha Q\left(\sqrt{2/\alpha E}\right)}. \quad (24)$$

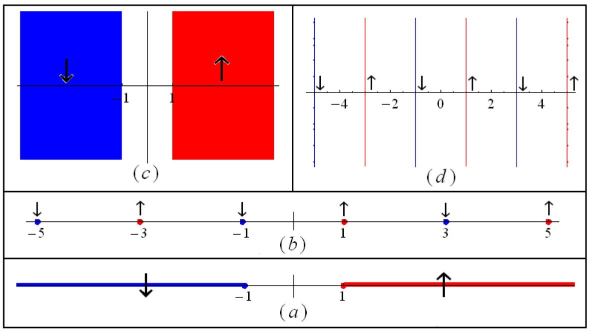

Fig. 1. Alphabet relaxation for BPSK.

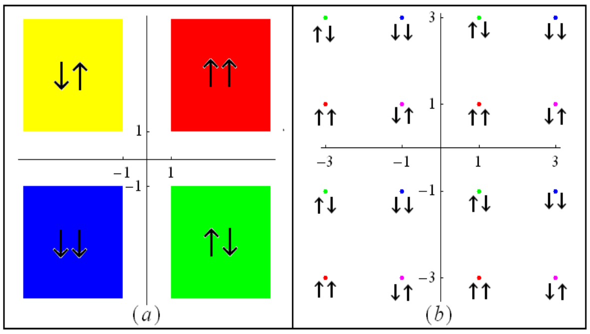

Fig. 2. Alphabet relaxation for QPSK.

C. One-dimensional binary lattice relaxation

Although the process of obtaining $\mathbf{x}$ from Eq. (17) is easier for convex alphabets, one might also relax BPSK alphabets in a discrete fashion. One possibility is using equispaced integer lattices:

$$\mathcal{A}_\uparrow = -\mathcal{A}_\downarrow = \{+1, -3, +5, -7, +9, \dots\}\,. \tag{25}$$

These extended alphabets, shown in Fig. 1.b, correspond to Tomlinson-Harashima precoding (see [16], [17]). The transmitted energy (19) reduces to

$$E = \frac{2\left\{\gamma_1^L\right\}^2 - 16\sum_{i=2}^{L}\gamma_{4i-5}^L Q\left(-\gamma_{4i-5}^L\sqrt{2/\alpha E}\right)}{2 - \tau\alpha + 8\sqrt{\frac{\alpha}{\pi E}}\sum_{i=2}^{L}\exp\left(-\left\{\gamma_{4i-5}^L\right\}^2/\alpha E\right)}, \tag{26}$$

where the index L is the size of the extended alphabet, *i.e.* the number of distinct elements in $\mathcal{A}_\uparrow$, and

$$\gamma_i^L \equiv 2L - i. \tag{27}$$

D. Binary semi-discrete relaxation

In [3] they proposed a trivial way to extend (25) onto the complex plane by adding an arbitrary purely imaginary component to the alphabet symbols (see Fig. 1.d). The transmitted energy (19) becomes

$$E = \frac{2\left\{\gamma_1^L\right\}^2 + \alpha E - 16\sum_{i=2}^{L}\gamma_{4i-5}^L Q\left(-\gamma_{4i-5}^L\sqrt{2/\alpha E}\right)}{2 + 8\sqrt{\frac{\alpha}{\pi E}}\sum_{i=2}^{L}\exp\left(-\left\{\gamma_{4i-5}^L\right\}^2/\alpha E\right)}, \tag{28}$$

where L the is number of distinct real parts in $\mathcal{A}_\uparrow$.

V. Alphabet Relaxation for Quaternary Phase Shift Keying (QPSK)

For purposes of comparison, we also consider a source of information consisting of four equiprobable states: $\uparrow\uparrow$, $\uparrow\downarrow$, $\downarrow\downarrow$ and $\downarrow\uparrow$. When no vector precoding is employed the entries in $\mathbf{x}$ are usually selected from the unit QPSK alphabets $\mathcal{A}_{\uparrow\uparrow} = \{1+j\}$, $\mathcal{A}_{\uparrow\downarrow} = \{1-j\}$, $\mathcal{A}_{\downarrow\downarrow} = \{-1-j\}$ and $\mathcal{A}_{\downarrow\uparrow} = \{-1+j\}$. Just as we did for the BPSK alphabets in Section IV, we might add points to these sets with the aim of reducing the transmitted energy.

In this section, the purely real BPSK relaxations introduced in Sections IV-A and IV-C are symmetrically extended onto the complex plane and proposed for relaxing QPSK modulation. The optimization is to be independently carried out on the real and imaginary dimensions.

As the alphabets we present in this section contain complex symbols, the vector precoding technique to be employed results in the energy metric $\mathbf{E}_\mathcal{C}$. This means that the parameter τ introduced in Section III is set equal to 2.

A. Quaternary convex relaxation

In [3] they proposed a quaternary extension of the relaxation scheme introduced in Section IV-A. Independent optimization is now carried out on the real and imaginary dimensions. The extended quaternary alphabets, shown in Fig. 2.a, are

$$\begin{aligned}\mathcal{A}_{\uparrow\uparrow} &= -\mathcal{A}_{\downarrow\downarrow} = \{\xi : \Re\xi \geq 1 \;\&\; \Im\xi \geq 1\}\,,\\ \mathcal{A}_{\uparrow\downarrow} &= -\mathcal{A}_{\downarrow\uparrow} = \{\xi : \Re\xi \geq 1 \;\&\; \Im\xi \leq -1\}\,.\end{aligned} \tag{29}$$

For an analysis of the probability that a typical such relaxed vector can be found in $\mathcal{S}_\mathbf{H}$ the reader is referred to [18].

The energy per transmitted symbol, given by (19), becomes

$$E = \frac{2 + \sqrt{\frac{\alpha E}{\pi}}\mathrm{e}^{-\Gamma^2} + \{\alpha E - 2\}\,Q\left(\sqrt{2/\alpha E}\right)}{1 - \alpha + 2\alpha Q\left(\sqrt{2/\alpha E}\right)}. \tag{30}$$

B. Quaternary lattice relaxation

A complex generalization of the one-dimensional discrete lattice introduced in Section IV-C was proposed in [3]. The QPSK unit alphabets are extended with a two-dimensional square lattice where independent optimization is carried out on the real and imaginary components. The resulting alphabets, shown in Fig. 2.b, are as follows:

$$\begin{aligned}\mathcal{A}_{\uparrow\uparrow} &= -\mathcal{A}_{\downarrow\downarrow} = \left\{\xi : \xi = 1 + 2n + j(1+2m)\ \forall (n,m) \in \mathbb{Z}^2\right\},\\ \mathcal{A}_{\uparrow\downarrow} &= -\mathcal{A}_{\downarrow\uparrow} = \left\{\xi : \xi = 1 + 2n - j(1+2m)\ \forall (n,m) \in \mathbb{Z}^2\right\},\end{aligned} \tag{31}$$

and the transmitted energy per symbol (19) reduces to

$$E = \frac{2\left\{\gamma_1^L\right\}^2 - 16\sum_{i=2}^{L}\gamma_{4i-5}^L Q\left(-\gamma_{4i-5}^L\sqrt{2/\alpha E}\right)}{1 - \alpha + 8\sqrt{\frac{\alpha}{\pi E}}\sum_{i=2}^{L}\exp\left(-\left\{\gamma_{4i-5}^L\right\}^2/\alpha E\right)}. \tag{32}$$

where L is the number of distinct real (or imaginary) values the elements of the square alphabet $\mathcal{A}_{\uparrow\uparrow}$ may take.

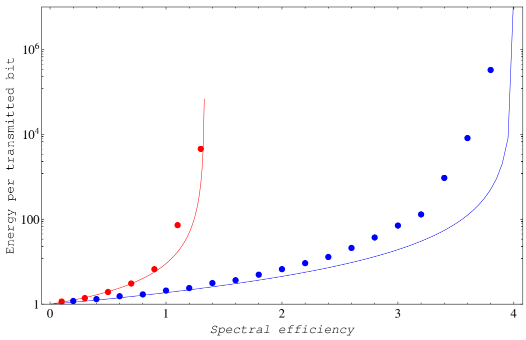

Fig. 3. Energy of vector precoding with the binary real convex relaxation shown in Fig. 1.*a*: using $\mathbf{T}_\mathcal{C}$ (red curve) and using $\mathbf{T}_\mathcal{R}$ (blue curve). The blue curve also represents the binary complex convex relaxation shown in Fig. 1.*c* and the quaternary convex relaxation shown in Fig. 2.*a*. The dots alongside the curves are from finite size simulations with $N = 10$ antennas at the transmitter.

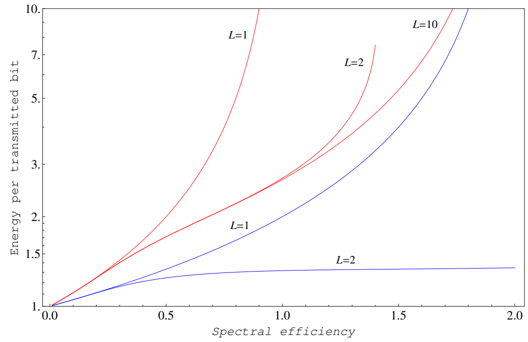

Fig. 4. Energy of vector precoding with the one-dimensional binary lattice relaxation shown in Fig. 1.*b*: using $\mathbf{T}_\mathcal{C}$ (red curves) and using $\mathbf{T}_\mathcal{R}$ (blue curves). The blue curves also represent the binary semi-discrete relaxation shown in Fig. 1.*d* and the quaternary lattice relaxation shown in Fig. 2.*b*. The curves for $L > 1$ are lower bounds resulting from the replica symmetric assumption. The $L = 1$ curves (exact results without lattice relaxations) are an upper bound for all other curves.

VI. Results

Fig. 3 shows the energy per transmitted bit vs. spectral efficiency (bits per transmitting antenna) for the binary real convex relaxation shown in Fig. 1.*a*. Although our analysis pertains to the asymptotic limit, finite size simulations show that the replica symmetric results can be used to approximate finite systems with as few as 10 transmitters. When $\mathbf{T}_\mathcal{C}$ is used, the channel is fully invertible only up to 1 bit/antenna, and it might be overloaded up to 1.33 bits/antenna. However, when $\mathbf{T}_\mathcal{R}$ is employed, the channel is fully invertible up to 2 bits/antenna, and it can support loads of up to 4 bits/antenna. As a result, precoding with $\mathbf{T}_\mathcal{R}$ results in lower energies than when $\mathbf{T}_\mathcal{C}$ is used. Indeed the use of $\mathbf{T}_\mathcal{R}$ makes optimization over a purely real convex space perform as well as the complex extension shown in Fig. 1.*c*. Also, the performance is similar to that of the quaternary convex relaxation shown in Fig. 2.*a*.

Fig. 4 shows the energy per transmitted bit vs. spectral efficiency for the binary lattice relaxation shown in Fig. 1.*b*. The replica symmetric assumption has recently been shown to break down and provide only an asymptotically loose lower bound to the actual energy of discrete alphabets [19]. However, the curves corresponding to the unperturbed lattice ($L = 1$) are asymptotically exact and they are an upper bound to any energy which might result from a discrete alphabet relaxation. As we can see in Fig. 4, precoding with $\mathbf{T}_\mathcal{C}$, as proposed in [3], results in higher energies than if one employs $\mathbf{T}_\mathcal{R}$. Indeed using $\mathbf{T}_\mathcal{R}$ with the unperturbed lattice (zero combinatorial complexity) draws less energy than any perturbed lattice under $\mathbf{T}_\mathcal{C}$. Using $\mathbf{T}_\mathcal{R}$ makes optimization over a purely real lattice perform as well as the complex extension shown in Fig. 1.*d*. The energy vs. spectral efficiency tradeoff is also similar to that of the quaternary lattice relaxation in Fig. 2.*b*.

References

[1] C. Windpassinger, R. F. H. Fischer, T. Vencel, and J. B. Huber, "Precoding in multiantenna and multiuser communications," *IEEE Trans. Wireless Commun.*, vol. 3(4), pp. 1305–1316, 2004.

[2] B. M. Hochwald, C. Peel, and A. Swindlehurst, "A vector-perturbation technique for near-capacity multiantenna multiuser communication-part II: Perturbation," *IEEE Trans. Commun.*, vol. 53(3), pp. 537–544, Mar. 2005.

[3] R. R. Müller, D. Guo, and A. Moustakas, "Vector precoding for wireless MIMO systems and its replica analysis," *IEEE J. Select. Areas Commun.*, vol. 26, pp. 530–540, Apr. 2008.

[4] A. M. Tulino and S. Verdú, "Asymptotic analysis of improved linear receivers for BPSK-CDMA subject to fading," *IEEE J. Select. Areas Commun.*, vol. 19, pp. 1544–1555, Aug. 2001.

[5] A. Lampe and M. Breiling, "Asymptotic analysis of widely linear MMSE multiuser detection - complex vs real modulation," in *Proc. of IEEE Information Theory Workshop (ITW), Cairns, Australia*, Sep. 2001.

[6] R. Schober, W. H. Gerstacker, and L. Lampe, "On suboptimum receivers for DS-CDMA with BPSK modulation," *Signal Processing*, vol. 85, pp. 1149–1163, 2005.

[7] W. Greiner, H. Stocker, and L. Neise, *Thermodynamics and Statistical Mechanics (Classical Theoretical Physics)*. Springer, 2004.

[8] K. Fischer, G. Parisi, and M. A. Virasoro, *Spin Glass Theory and Beyond*. World Scientific, 1987.

[9] A. Turiel, E. Korutcheva, and N. Parga, "The mutual information of a stochastic binary channel: validity of the replica symmetry ansatz," *J. Phys. A: Math. Gen.*, vol. 32, pp. 1875–1894, 1999.

[10] T. Tanaka, "A statistical mechanics approach to large-system analysis of CDMA multiuser detectors," *IEEE Trans. Inform. Theory*, vol. 48, pp. 2888–2910, Nov. 2002.

[11] A. L. Moustakas, S. H. Simon, and A. M. Sengupta, "MIMO capacity through correlated channels in the presence of correlated interferers and noise: A (not so) large n analysis," *IEEE Trans. Inform. Theory*, vol. 49, Oct. 2003.

[12] R. R. Müller and W. H. Gerstacker, "On the capacity loss due to separation of detection and decoding," *IEEE Trans. Inform. Theory*, vol. 50, pp. 1769–1778, Aug. 2004.

[13] D. Guo and S. Verdú, "Randomly spread CDMA: Asymptotics via statistical physics," *IEEE Trans. Inform. Theory*, vol. 51, pp. 1983–2010, Jun. 2005.

[14] Y. Kabashima and D. Saad, "Statistical mechanics of error-correcting codes," *Europhysics Letters*, vol. 45, 1999.

[15] A. Montanari and N. Sourlas, "The statistical mechanics of turbo codes," *The European Physics Journal B*, vol. 18, pp. 107–119, 2000.

[16] M. Tomlinson, "New automatic equaliser employing modulo arithmetic," *IEE Elec. Lett.*, vol. 7, pp. 138–139, Mar. 1971.

[17] H. Harashima and H. Miyakawa, "Matched-transmission technique for channels with intersymbol interference," *IEEE Trans. Commun.*, vol. COM-20, pp. 774–780, Aug. 1972.

[18] V. Gardasevic, R. R. Müller, and F. F. Knudsen, "Vector precoding for singular MIMO channels," *Submitted to IEEE International Symposium on Information Theory and its Applications (ISITA), Auckland, New Zeeland, 2008*.

[19] B. M. Zaidel, R. R. Müller, R. de Miguel, and A. L. Moustakas, "On spectral efficiency of vector precoding for gaussian MIMO broadcast channels," in *Proc. of IEEE International Symposium on Spread Spectrum Techniques and Applications (ISSSTA), Bologna, Italy*, Aug. 2008.